ARTHRITIS & RHEUMATISM
Vol. 65, No. 11, November 2013, pp 2835–2846
DOI 10.1002/art.38124

Lipopolysaccharide Increases the Incidence of Collagen-Induced Arthritis in Mice Through Induction of Protease HTRA-1 Expression

Yuzhu Hou,[1] Haijiang Lin,[2] Linnan Zhu,[1] Zhaoting Liu,[1] Fanlei Hu,[3] Jianfeng Shi,[1] Tao Yang,[1] Xiaoyun Shi,[4] Mingzhao Zhu,[5] Bernard F. Godley,[2] Qiang Wang,[1] Zhanguo Li,[3] and Yong Zhao[1]

Objective. **The protease HTRA-1 is closely associated with rheumatoid arthritis (RA). The molecular mechanisms that control HTRA-1 expression are currently unknown. This study was undertaken to determine the regulatory role of Toll-like receptors (TLRs) on HTRA-1 expression in mice with collagen-induced arthritis (CIA) and in synovial cells from RA patients.**

Methods. **HTRA-1 messenger RNA and protein production in mouse fibroblasts, mouse macrophages, and freshly isolated RA patient synovial cells treated with TLR ligands were detected by real-time polymerase chain reaction and enzyme-linked immunosorbent assay, respectively. Arthritis incidence and severity were determined using clinical scores and histopathologic analysis. Involvement of HTRA-1 in lipopolysaccharide (LPS)–increased arthritis incidence and severity in mice was determined using anti–HTRA-1 monoclonal antibody. The signal pathways involved in HTRA-1 expression were accessed by specific inhibitors, RNA interference, dual-luciferase reporter, and chromatin immunoprecipitation methods.**

Results. **LPS and tenascin-C, but not the other TLR ligands tested, strongly induced HTRA-1 expression. LPS significantly increased HTRA-1 expression in the joint tissue as well as arthritis incidence and severity in mice with CIA. Blocking HTRA-1 by antibody significantly decreased LPS-promoted CIA severity. Inhibiting NF-κB significantly decreased LPS-induced HTRA-1 expression in mouse and human cells. Dual-luciferase reporter assay and ChIP analysis showed that p65 directly binds to HTRA-1 promoter (amino acid 347).**

Conclusion. **Our findings indicate that TLR-4 activation increases HTRA-1 expression through the NF-κB pathway in fibroblasts and macrophages. HTRA-1 expression is involved in the enhancing effects of LPS on CIA. This study offers new insights into the regulation of HTRA-1 expression via LPS/TLR-4 and the role of HTRA-1 in RA pathogenesis.**

Rheumatoid arthritis (RA) is a common autoimmune disease with a prevalence of ~1% worldwide. RA is characterized by chronic inflammation and high levels of destructive mediators in the synovium, which leads to cartilage and bone destruction (1). Bacterial and viral infections are associated with the occurrence and pathogenesis of RA flares (2–3). The critical involve-

Supported by the National Basic Research Program of China (grants 2010CB945301 and 2011CB710900 to Dr. Zhao and grant 2010CB529100 to Dr. Li) and the National Natural Science Foundation for General and Key Programs (grants C81130055 and U0832003 to Dr. Zhao).

[1]Yuzhu Hou, PhD, Linnan Zhu, BS, Zhaoting Liu, PhD, Jianfeng Shi, MS, Tao Yang, PhD, Qiang Wang, PhD, Yong Zhao, MD, PhD: State Key Laboratory of Biomembrane and Membrane Biotechnology, Institute of Zoology, and Chinese Academy of Sciences, Beijing, China; [2]Haijiang Lin, MD, PhD, Bernard F. Godley, MD: University of Texas Medical Branch, Galveston; [3]Fanlei Hu, MD, PhD, Zhanguo Li, MD, PhD: Clinical Immunology Center and Peking University People's Hospital, Beijing, China; [4]Xiaoyun Shi, MD, PhD: State Key Laboratory of Biomembrane and Membrane Biotechnology, Institute of Zoology, Chinese Academy of Sciences, and General Hospital of Chinese People's Armed Police Forces, Beijing, China; [5]Mingzhao Zhu, PhD: Institute of Biophysics and Chinese Academy of Sciences, Beijing, China.

Drs. Hou and Lin contributed equally to this work. Ms L. Zhu and Drs. Liu and Hu contributed equally to this work.

Address correspondence to Yong Zhao, MD, PhD, or Qiang Wang, PhD, State Key Laboratory of Biomembrane and Membrane Biotechnology, Institute of Zoology, Chinese Academy of Sciences, Beichen West Road 1-5, Chaoyang District, Beijing, China 100101 (e-mail: zhaoy@ioz.ac.cn or qiangwang@ioz.ac.cn); or to Zhanguo Li, MD, PhD, Department of Rheumatology and Immunology, Clinical Immunology Center, Peking University People's Hospital, 11 Xizhimen South Street, Beijing, China 100044 (e-mail: zgli@yahoo.cn).

Submitted for publication November 25, 2012; accepted in revised form August 1, 2013.

ment of Toll-like receptors (TLRs) activated by exogenous and endogenous ligands in the initiation and persistence of inflammation in RA is currently recognized (4–7). A number of studies have identified the presence of endogenous TLR ligands in the synovial tissue of patients with RA, including tenascin, fibrinogen, Hsp60, Hsp70, Hsp22, and fragments of hyaluronic acid (8–9). In particular, tenascin-C (TN-C), an extracellular matrix (ECM) glycoprotein specifically expressed in areas of inflammation and tissue damage, has been shown to be an endogenous activator of TLR-4–mediated immunity, which is involved in persistent synovial inflammation and tissue destruction in arthritic joint disease (10). Although these studies have significantly improved our understanding of the role of TLRs in RA, further insight is required to delineate the molecular mechanisms by which infection and TLRs cause joint tissue destruction.

HTRA-1 (PRSS11 or L56) is a secreted serine protease that has a highly conserved trypsin-like protease domain and a C-terminal PDZ domain (11). The role of HTRA-1 in degrading proteins such as fibronectin, aggrecan, decorin, biglycan, fibromodulin, nidogen 1 and 2 (structural constituents of basement membranes), E-cadherin, talin, fascin, chloride intracellular channel 1, and transforming growth factor β family members (12–18) makes it central to ECM homeostasis and turnover, intercellular adhesion, and cell migration. In humans, elevated HTRA-1 levels have been associated with RA, osteoarthritis (OA), age-related macular degeneration (AMD), Duchenne's muscular dystrophy, and aging (19–25). Locally enhanced HTRA-1 may be one of the key mediators in arthritic diseases, since it directly degrades cartilage through proteolytic cleavage of ECM components and stimulates overproduction of matrix metalloproteinase (MMP) by synovial fibroblasts (12,13,20,26). In contrast, decreased HTRA-1 expression contributes to the aggressiveness, metastatic ability, and chemoresistance of tumors (23,27). However, the microenvironmental extracellular factors and intracellular upstream events that regulate HTRA-1 expression in mammalian cells were previously unknown.

In this study, we discovered that TLR-4 ligands efficiently induced HTRA-1 expression in fibroblasts and macrophages. The relationship between TLR-4 ligands and HTRA-1 expression was also observed in mouse models of RA and in humans with RA. These observations offer new insights into the molecular pathophysiology of RA and the interaction of infection and inflammation with mediators of tissue destruction. These findings may have a significant impact on the development of new clinical treatments for RA and other HTRA-1–related processes, such as OA, AMD, cancer, and aging.

MATERIALS AND METHODS

Animals and reagents. C57BL/6 mice were purchased from Beijing University Experimental Animal Center. All mice were maintained in a specific pathogen–free facility and were housed in microisolator cages containing sterilized feed, autoclaved bedding, and water. All experiments were undertaken in accordance with the Institutional Guidelines for the Care and Use of Laboratory Animals, Institute of Zoology.

A mouse TLR1–9 agonist kit was purchased from InvivoGen. Bacterial lipopolysaccharide (LPS; *Escherichia coli* O55:B5) was purchased from Sigma-Aldrich. The p38 MAPK inhibitor SB203580, the phosphatidylinositol 3-kinase (PI3K) inhibitor LY294002, and the NF-κB inhibitor 6-AQ were acquired from Merck. The JNK inhibitor SP600125 and the ERK inhibitor U0126 were from Sigma-Aldrich. The NF-κB inhibitor celastrol was from Invitrogen. Human TN-C and HTRA-1 were obtained from R&D Systems.

Except where indicated otherwise, the reagents were used at the following concentrations: 500 ng/ml of the TLR-1/2 agonist palmitoyl-3-cysteine-serine-lysine-4 (Pam_3CSK_4), 10^8 cells/ml of the TLR-2 agonist HKLM, 1 μg/ml of the TLR-3 agonist poly(I-C), 500 ng/ml of the TLR-4 agonist LPS-EK (LPS preparation with *E coli* K12), 100 ng/ml of the TLR-5 agonist ST-FLA (standard flagellin from *Salmonella typhimurium*), 100 ng/ml of the TLR-6/2 agonist fibroblast-stimulating lipopeptide 1 (FSL-1), 1 μg/ml of the TLR-7 agonist ssRNA40/LyoVec; 5 μM TLR-9 agonist ODN1826; 10 μM p38 MAPK inhibitor SB203580, 1 μM PI3K inhibitor LY294002, 10 μM JNK inhibitor SP600125, 5 μM celastrol, and 10 nM of Merck NF-κB inhibitor.

Cells. Freshly isolated mouse macrophages were obtained from peritoneal exudates as previously described (28), and the purity was confirmed by flow cytometry using anti-F4/80 and anti-CD11b monoclonal antibodies (mAb; Tianjin Sungene Biotech). Mouse embryonic fibroblasts (MEFs) were isolated in our laboratory. RAW 264.7 (TIB-71), a murine macrophage-like cell line, was purchased from ATCC. Human synovial cells from RA patients were provided by Professor Li Zhanguo (People's Hospital, Peking University). Cells were cultured in Dulbecco's modified Eagle's medium (DMEM; HyClone) containing 10% fetal bovine serum and 1% penicillin/streptomycin at 37°C under 5% CO_2.

Immunofluorescence staining. Cells were cultured on coverslips for the indicated times and then fixed in 4% paraformaldehyde for 10 minutes and stored in phosphate buffered saline (PBS) at 4°C. Cells were permeabilized in 0.2% Triton X-100/PBS for 10 minutes at room temperature and blocked for 1 hour in 5% bovine serum albumin (BSA)/PBS. Cells were incubated in a BSA/PBS solution containing the indicated mAb (1:100 dilution in blocking buffer) overnight at 4°C. Following PBS washes, secondary antibody (Alexa Fluor 546–conjugated goat anti-rabbit antibody, 1:500 dilution; Invitrogen) was applied for 1 hour, and Hoechst 33342 (2 μg/ml) was applied for 10 minutes before the coverslips were washed in PBS and mounted. Photomicrographs were

taken using an LSM 510 META laser scanning microscope (Zeiss).

Western blotting. Western blotting of total cell lysates and immunoblot analysis were performed as previously described (29). Protein bands were visualized by adding horseradish peroxidase (HRP) membrane substrate (Millipore) and then scanned using a Tanon 1600R Gel Image System. The following antibodies were used: anti–HTRA-1 (sc-50335; Santa Cruz Biotechnology), anti–phospho-p38 MAPK (9211), anti–p38 MAPK (9218), anti–phospho–ERK-1/2 (9101), anti–ERK-1/2 (4695), anti–phospho-JNK (Thr^{183}/Tyr^{185}; 4668), anti-JNK (9252), anti–phospho-AKT (Ser^{473}; 9271), and anti-AKT (9272) (all from Cell Signaling Technology), and anti–tuberous sclerosis complex 2 (TSC-2; Epitomics). The amount of loaded protein was normalized to GAPDH mAb (Proteintech Group).

Enzyme-linked immunosorbent assay (ELISA) to detect HTRA-1. HTRA-1 protein levels in synovial fluid and culture media were determined using ELISA. Briefly, ELISA plates were coated overnight with the anti–HTRA-1 antibody SAB1300009 (1:200 dilution; Sigma-Aldrich) and blocked with 5% BSA/PBS. Plates were washed with 0.05% PBS–Tween and incubated with samples for 2 hours at 30°C. After washing, the anti–HTRA-1 antibody sc-15465 (1:100 dilution; Santa Cruz Biotechnology) was added for 1 hour at 30°C followed by HRP-conjugated donkey anti-goat IgG (sc-2020, 1:5,000 dilution; Santa Cruz Biotechnology) for 1 hour at 30°C. Plates were developed using 3,3′,5,5′-tetramethylbenzidine in 100 m*M* citric acid, 0.1% H_2O_2, pH 3.95. The reaction was stopped with 2*M* H_2SO_4, and optical densities were determined at 450 nm using a plate reader. Purified recombinant HTRA-1 (2916SE; R&D Systems) was tested at concentrations ranging from 1 ng/ml to 128 ng/ml to generate a standard curve.

Real-time polymerase chain reaction (PCR) for HTRA-1 messenger RNA (mRNA). TRIzol was used to isolate mRNA according to the recommendations of the manufacturer (Invitrogen). A real-time PCR kit (SYBR Premix Ex Taq, DRR041A) was purchased from Takara Bio. PCR was performed using a Bio-Rad CFX96 system. The housekeeping gene hypoxanthine guanine phosphoribosyltransferase (HPRT) was used as an internal control. The following primer pairs were used: for human HPRT, forward 5′-CAGTATAATCCAAAGATGGTCAA-3′ and reverse 5′-TTAGGCTTTGTATTTTGCTTTTCC-3′; for human HTRA-1, forward 5′-CAAGGATGTGGATGAGAAAGCAGACA-3′ and reverse 5′-ATGATGGCGTCGGTCTGGATGTAGTC-3′; for mouse HPRT, forward 5′-AGTACAGCCCCAAAATGGTTAAG-3′ and reverse 5′-CTTAGGCTTTGTATTTGGCTTTTC-3′; for mouse HTRA-1, forward 5′-CAAGGATGTGGATGAAAAGGC-3′ and reverse 5′-ATGATAGCGTCTGTCTGAATGTAGTC-3′; and for mouse MMP-3, forward 5′-TGATGAACGATGGACAGAGGAT-3′ and reverse 5′-AAACGGGACAAGTCTGTGGAG-3′.

Induction and assessment of collagen-induced arthritis (CIA). CIA was induced in twelve 14-week-old male B6 mice by injection of chicken type II collagen (C9301; Sigma-Aldrich) (30). Mice were treated with intraperitoneal injections of LPS (30 μg) on day 23. Some of the mice also received an intravenous injection of anti–HTRA-1 antibody (100 μg; Santa Cruz Biotechnology) on day 23.

Mice were assessed macroscopically for arthritis by using microcalipers to measure the thickness of the hind paw 2–3 times per week. The average hind paw thickness of the mice with arthritis in each group was calculated. The reported diameter was an average of the inflamed hind paws per mouse. Animals were also scored for clinical signs of arthritis on a scale of 0–3 (31), where 0 = normal, 1 = slight swelling and/or erythema, 2 = pronounced edematous swelling, and 3 = joint rigidity. Each limb was graded, allowing a maximum score of 12 per mouse. At the end of the experiment, the hind paws of the mice were removed, fixed, decalcified with EDTA (150 gm/liter, pH 7.5), and paraffin embedded. Sections (5 μm) were stained with hematoxylin and eosin and examined for histologic changes of inflammation, pannus formation, and cartilage as well as bone damage.

DNA transfection. RAW 264.7 cells were grown overnight to obtain 70–80% confluent monolayer cells in 24-well plates. DNA plasmids (0.2–0.5 μg) were transfected using Lipofectamine 2000 transfection reagent (Invitrogen) according to the manufacturer's protocol. Opti-MEM I (50 μl) and Lipofectamine 2000 (1.5 μl) were incubated for 5 minutes at room temperature. DNA (0.2–0.5 μg) was added to the mixture and incubated for an additional 20 minutes. After the medium was removed, the DNA mixture and Opti-MEM I (250 μl) were then added to each well and incubated at 37°C for 4 hours. Subsequently, complete DMEM (1 ml) was added to the mixture. Transfected cells were then incubated for 24–72 hours in the medium (1.3 ml). The cells were then processed to be used in assays.

Dual-luciferase reporter assay. Dual-luciferase reporter assays were performed as previously described (32). RAW 264.7 cells (4×10^5 cells per well in 24-well plates) were cotransfected with expression plasmid DNA (0.1–0.3 μg), Fluc reporter plasmid (0.1 μg), and the internal control vector pRL-TK (0.1 μg) using Lipofectamine 2000 transfection reagent according to the manufacturer's protocol. Twenty-four hours after transfection, the cells were stimulated with the described reagents for another 24 hours and then collected, lysed with 50 μl 1× passive lysis buffer, and subsequently assayed for luciferase activity using a Dual-Luciferase Reporter Assay system (E1910; Promega).

Chromatin immunoprecipitation (ChIP) assay. ChIP assays were performed using $\sim 2 \times 10^7$ RAW 264.7 cells, according to a previously described protocol, with slight modifications (18). Briefly, cells were crosslinked with 1% formaldehyde for 10 minutes at room temperature, and the reaction was quenched by the addition of glycine to a final concentration of 0.125*M*. Chromatin was sonicated to an average size of 0.5–1 kb, using a Bioruptor system (Diagenode). A total of 3–5 μg of anti-p65 antibody (catalog no. 3987; CST) was added to the sonicated chromatin and incubated overnight at 4°C. Of the chromatin used for each ChIP reaction, 10% was kept as input DNA. Subsequently, 75 μl of protein A or protein G Dynal magnetic beads were added to the ChIP reactions and incubated for an additional 4 hours at 4°C. Magnetic beads were washed and chromatin was eluted, followed by reversal of the crosslinkings and DNA purification. The resultant ChIP DNA was dissolved in water. ChIP DNA was then used as a template for PCR using the following primers: for NF-κB binding site 1, forward 5′-CCACGGCGGCGTCAAGTTCA-3′ and reverse 5′-TGGCTCAGTTTCTCATTCTA-3′; for NF-κB binding site 2, forward 5′-CCCCTTGATGTGTGGGACTT-3′ and reverse 5′-GCACCTCGCCATAACACACC-3′; and for

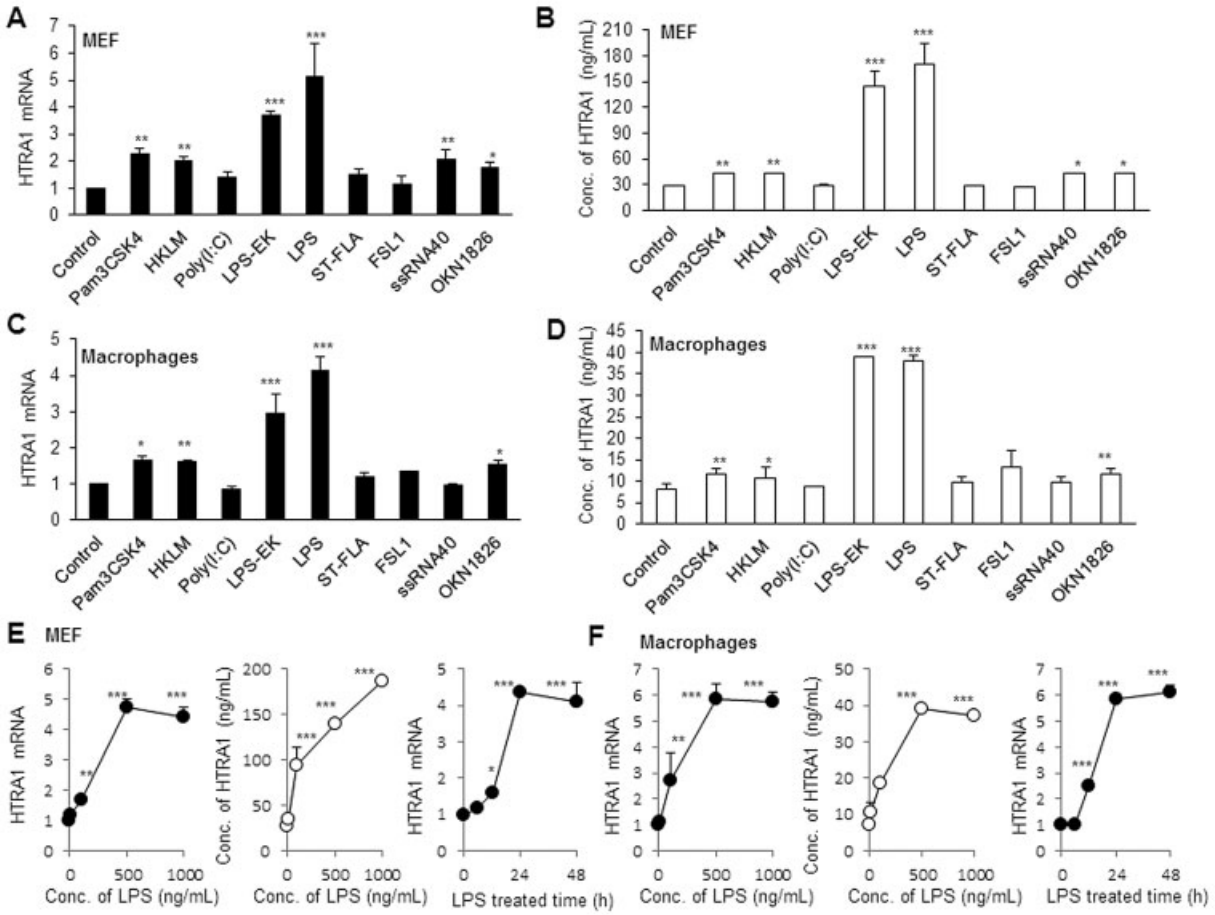

Figure 1. Effects of Toll-like receptor (TLR) ligands on HTRA-1 expression in mouse embryonic fibroblasts (MEFs) and mouse macrophages. **A–D**, Levels of HTRA-1 mRNA (**A** and **C**) and protein (**B** and **D**) in MEFs (**A** and **B**) and freshly isolated mouse macrophages (**C** and **D**) cultured with the indicated TLR ligands for 24 hours as described in Materials and Methods. HTRA-1 mRNA expression was determined by real-time polymerase chain reaction (PCR), and secreted HTRA-1 protein concentrations from the culture media were determined by enzyme-linked immunosorbent assay (ELISA). Pam_3CSK_4 = palmitoyl-3-cysteine-serine-lysine-4; LPS-EK = lipopolysaccharide preparation with *Escherichia coli* K12; ST-FLA = standard flagellin from *Salmonella typhimurium*; FSL-1 = fibroblast-stimulating lipopeptide 1. **E** and **F**, Levels of HTRA-1 mRNA and protein in MEFs (**E**) and mouse macrophages (**F**) cultured with different concentrations of LPS for 24 hours or with 500 ng/ml of LPS for different time periods. HTRA-1 mRNA expression was determined by real-time PCR, and HTRA-1 levels in the supernatant were assayed by ELISA. Values are the mean ± SD (n = 3 samples per group) and are representative of at least 3 independent experiments with similar results. $* = P < 0.05$; $** = P < 0.01$; $*** = P < 0.001$, versus controls in **A–D** and versus no LPS or 0 hours in **E** and **F**.

nonspecific binding site, forward 5′-GAACCAGAAGGAACACAAGC-3′ and reverse 5′-AATCCTCAGACTACAGAAAC-3′.

Statistical analysis. Data are presented as the mean ± SD. Student's unpaired *t*-test for comparison of means was used. *P* values less than 0.05 were considered significant.

RESULTS

Effects of TLR ligands on HTRA-1 expression in mouse macrophages and MEFs. In order to determine whether TLR signals regulate HTRA-1 expression in fibroblasts and macrophages, which are the major producers of HTRA-1 in RA (20), we analyzed HTRA-1 mRNA and protein expression after mouse macrophages and MEFs were stimulated with different ligands of TLRs, which have previously been demonstrated to be involved in RA progression (1,8). Among the TLR-1 through TLR-9 ligands tested, the TLR-4 ligands LPS and LPS-EK were the most potent inducers of HTRA-1 mRNA expression and protein release in MEFs, as determined by real-time PCR and ELISA ($P < 0.001$) (Figures 1A and B). Pam_3CSK_4 (TLR-1/2), HKLM

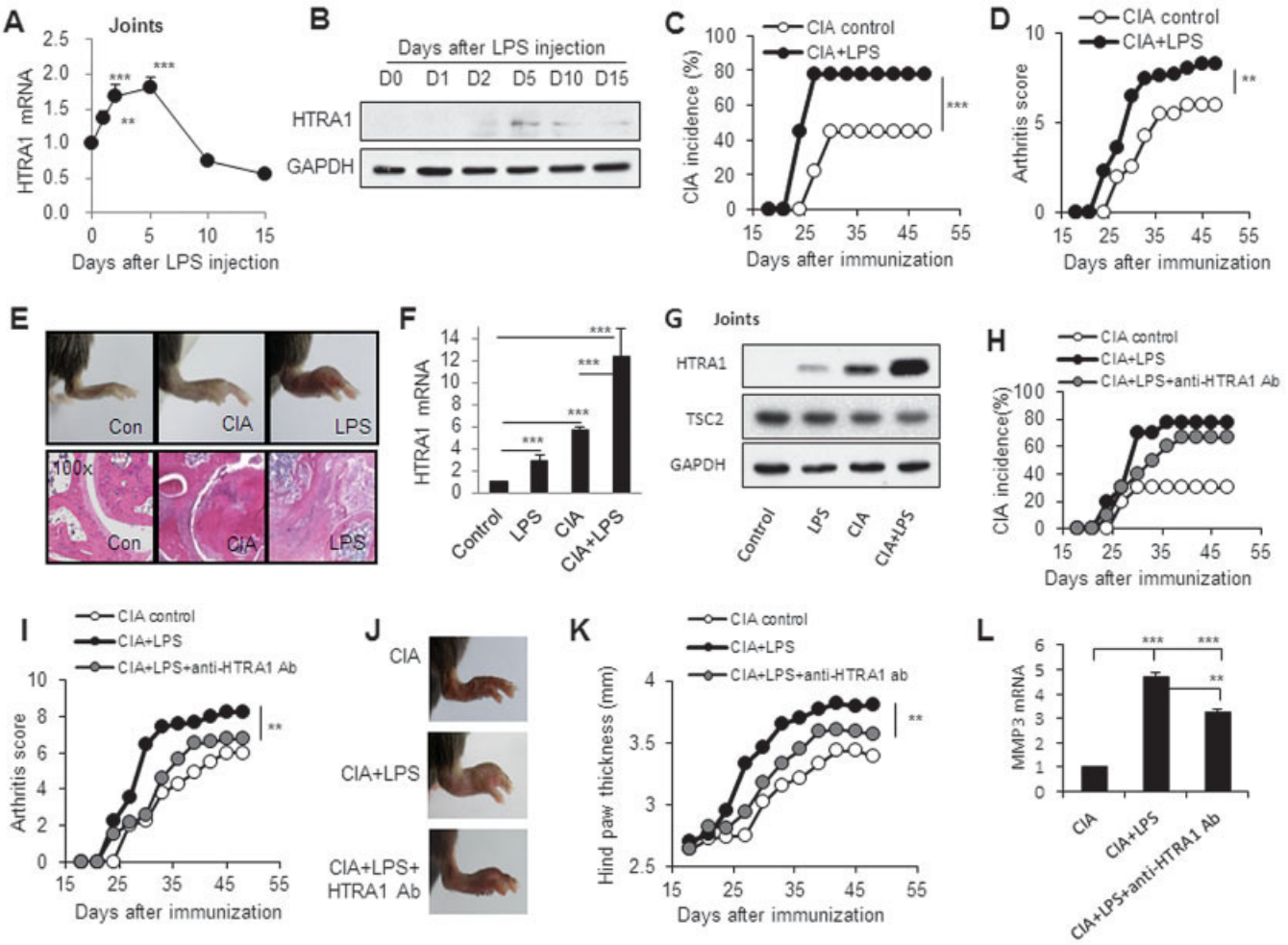

Figure 2. Regulation of HTRA-1 expression in normal mice and mice with collagen-induced arthritis (CIA) by TLR-4 ligands. **A** and **B**, HTRA-1 mRNA (**A**) and protein (**B**) expression in joint tissue from B6 mice determined on the indicated days after intraperitoneal injection of 50 μg of LPS (n = 4 mice per time point). HTRA-1 mRNA levels were determined by real-time PCR, and HTRA-1 protein levels were determined by Western blotting. **C–E**, CIA incidence (**C**), clinical scores (**D**), and imaging of the hind paws and hematoxylin and eosin–stained joint tissue (**E**) in B6 control mice with CIA and B6 mice with CIA treated with LPS (n = 9 mice per group). **F** and **G**, HTRA-1 mRNA expression (**F**) and HTRA-1 and tuberous sclerosis complex (TSC-2; HTRA-1 target molecule) protein expression (**G**) in joint tissue from control mice, mice treated with LPS, mice with CIA, and mice with CIA treated with LPS (n = 9 mice per group). HTRA-1 mRNA levels were determined by real-time PCR, and HTRA-1 protein levels were determined by Western blotting. **H–L**, CIA incidence (**H**), clinical scores (**I**), imaging of the hind paws (**J**), hind paw thickness (**K**), and expression of matrix metalloproteinase 3 (MMP-3) mRNA in joint tissue (**L**) in control mice with CIA, mice with CIA treated with LPS, and mice with CIA treated with LPS and anti–HTRA-1 antibody (Ab) (n = 10 mice per group). The expression of MMP-3 mRNA was determined by real-time PCR. Values in **A**, **F**, and **L** are the mean ± SD. Values in **D**, **I**, and **K** are the mean. ** = $P < 0.01$; *** = $P < 0.001$, versus day 0 in **A** and versus the indicated groups in **C**, **D**, **F**, **I**, **K**, and **L**. See Figure 1 for other definitions.

(TLR-2), ssRNA40 (TLR-7), and ODN1826 (TLR-9) slightly but significantly induced HTRA-1 expression in MEFs ($P < 0.05$) (Figures 1A and B), even at higher doses (data available from the corresponding authors upon request). Yet, poly(I-C) (TLR-3), ST-FLA (TLR-5), and FSL-1 (TLR-2/6) at different doses failed to promote HTRA-1 expression ($P > 0.05$) (Figures 1A and B) (data available from the corresponding authors upon request).

Consistent with our observations in MEFs, LPS efficiently promoted HTRA-1 mRNA and protein expression in mouse macrophages (Figures 1C and D). Other TLR ligands, including Pam_3CSK_4, HKLM, poly(I-C), ST-FLA, FSL-1, ssRNA40, and OKN1826

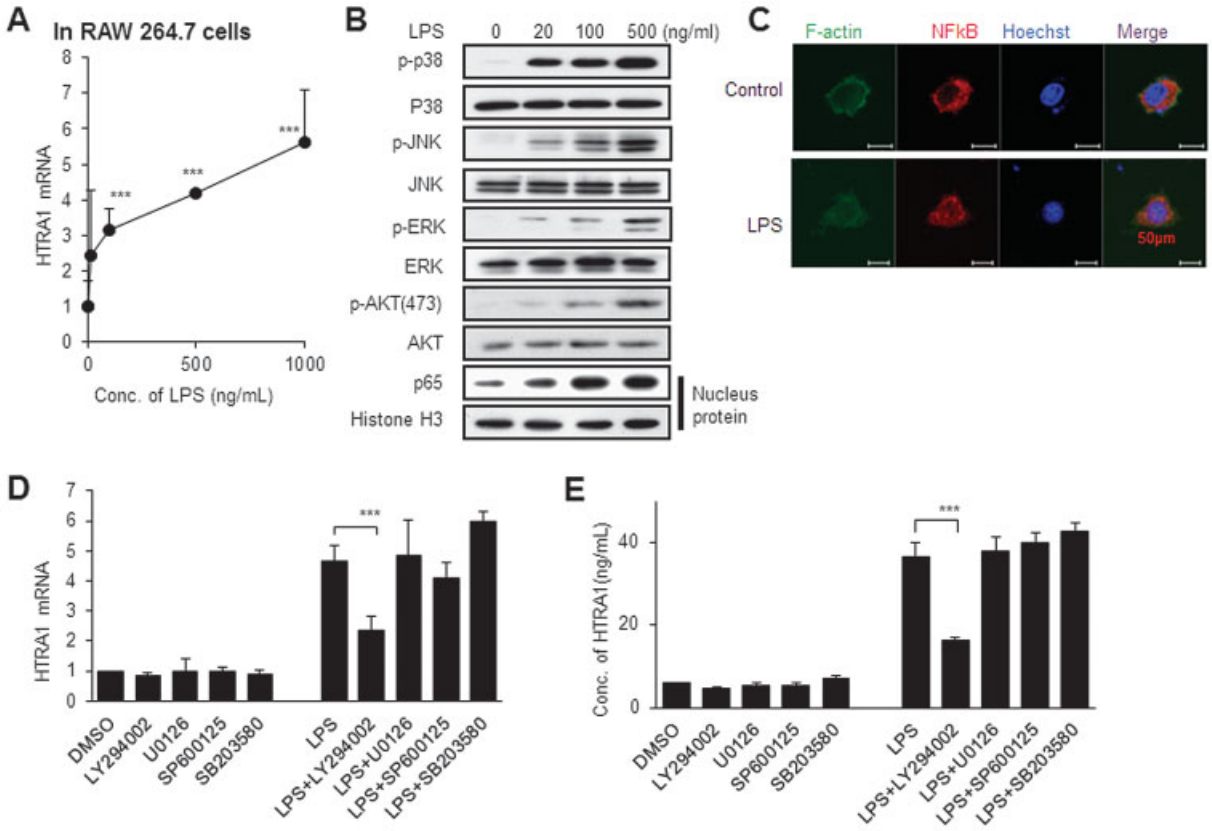

Figure 3. Phosphatidylinositol 3-kinase (PI3K) contributes to the lipopolysaccharide (LPS)–induced expression of HTRA-1 in mouse macrophages. **A**, HTRA-1 mRNA expression in RAW 264.7 cells cultured with the indicated concentrations of LPS for 24 hours. **B**, Western blot of the phosphorylation of p38, JNK, ERK, AKT, and nuclear p65 in RAW 264.7 cells cultured with LPS for 30 minutes at the indicated concentrations. **C**, Intracellular location of p65 in RAW 264.7 cells, detected using a dual-photon microscope 30 minutes after stimulation with LPS. **D** and **E**, HTRA-1 mRNA expression (**D**) and HTRA-1 protein concentrations in the culture medium (**E**) in RAW 264.7 cells pretreated with inhibitors of PI3K (LY294002), ERK (U0126), JNK (SP600125), and p38 MAPK (SB203580) for 30 minutes and cultured with LPS for an additional 24 hours. Values in **A**, **D**, and **E** are the mean ± SD (n = 3 samples per group) and are representative of at least 3 independent experiments with similar results. *** = $P < 0.001$ versus time 0 in **A**; versus the indicated groups in **D** and **E**.

either only slightly induced or did not induce HTRA-1 expression at different doses (Figures 1C and D) (data available from the corresponding authors upon request). Furthermore, the effects of LPS on HTRA-1 mRNA expression and protein secretion into the medium were dose- and time-dependent in MEFs and mouse macrophages (Figures 1E and F).

To examine the effect of LPS on HTRA-1 expression in vivo and the potential involvement of this pathway in RA pathogenesis, we first analyzed HTRA-1 expression in the joint tissue at different time points after intraperitoneal injection of LPS into normal B6 mice. Consistent with the in vitro results, LPS promoted significantly increased HTRA-1 mRNA and protein production in the joints of B6 mice, as determined by real-time PCR and Western blotting ($P < 0.001$) (Figures 2A and B). Thus, TLR-4 ligands were identified as important extracellular factors for controlling HTRA-1 expression in mouse fibroblasts and macrophages, the major cell types involved in HTRA-1 expression in RA (20). Additionally, the effects on HTRA-1 expression of tumor necrosis factor α (TNFα) and interleukin-1β (IL-1β), which can be induced by LPS and are involved in the pathologic process of RA, were investigated. TNFα and IL-1β did not significantly alter HTRA-1 expression in MEFs but seemed to decrease HTRA-1 expression in mouse macrophages (data available from the corresponding authors upon request). Thus, in the subsequent experiments, we focused on the role of LPS on HTRA-1 expression in models of RA.

Regulation of HTRA-1 expression in mice with CIA by TLR-4 ligands. In an effort to determine the clinical significance of these observations, we investigated the regulatory effects of LPS on HTRA-1 expres-

sion in a standard mouse model of CIA. We treated B6 mice with CIA with a low dose of LPS during CIA induction, as described in Materials and Methods. There was a higher incidence of CIA in the group of mice treated with a low dose of LPS ($P < 0.001$) (Figure 2C), and these mice had more severe arthritis than the control mice with CIA, as evaluated by clinical arthritis score (Figure 2D), hind paw thickness (Figure 2E), and histologic examination of tissue samples (Figure 2E). Consistent with observed arthritis severity patterns, joint tissue from mice with CIA that were injected with LPS expressed significantly higher HTRA-1 mRNA and protein levels than did mice with CIA that were not treated with LPS ($P < 0.001$) (Figures 2F and G). Thus, LPS regulated HTRA-1 production in mice with CIA. Levels of TSC-2 protein, one of the direct target molecules of HTRA-1 (33), were decreased in the joint tissue of mice with CIA treated with LPS compared with untreated mice with CIA (Figure 2G), supporting the notion of enhanced HTRA-1 activity in LPS-treated mice.

To assess whether LPS-induced HTRA-1 expression is involved in the pathologic process in the mouse model of CIA, we used an antibody to block HTRA-1 activity. The in vitro study showed that anti–HTRA-1 antibody (15465; Santa Cruz Biotechnology) decreased HTRA-1 activity as determined by its inhibiting effects on HTRA-1–induced expression of MMP-3 (data available from the corresponding authors upon request), which is one of the target molecules positively regulated by HTRA-1 (20). Thus, we used this antibody to block HTRA-1 activity in the animal model. Injection of anti–HTRA-1 mAb only slightly decreased the LPS-enhanced incidence of CIA (Figure 2H). However, injection of anti–HTRA-1 mAb partially, but significantly, decreased LPS-enhanced CIA symptoms, as evidenced by the decreased clinical arthritis score (Figure 2I) and hind paw thickness (Figures 2J and K) compared to LPS-treated mice with CIA that received control IgG treatment. Consistent with these findings, MMP-3 was also decreased by injection of anti–HTRA-1 mAb into the joint tissue of LPS-treated mice with CIA (Figure 2L). Thus, HTRA-1 expression is involved in LPS-enhanced arthritis pathogenesis in mice.

LPS induces HTRA-1 expression via the classical NF-κB pathway in mouse macrophages. Experiments were performed in an attempt to understand the intracellular signal pathways mediating the effects of LPS on HTRA-1 synthesis. The monocyte/macrophage cell line RAW 264.7 was a potential model cell line for these experiments. RAW 264.7 cells produced more HTRA-1 mRNA after LPS stimulation compared to unstimulated RAW 264.7 cells, as freshly isolated primary macrophages (Figure 3A). Therefore, the molecular and biochemical assays described below were performed mainly using RAW 264.7 cells.

In RAW 264.7 cells, LPS promoted significant phosphorylation of p38 MAPK, ERK, and AKT (protein kinase B) (Figure 3B), as previously described (34). LPS stimulation increased p65 levels in the nuclear fraction (Figure 3B). Nuclear localization of increased NF-κB after LPS stimulation was further confirmed by dual-photon confocal microscopy (Figure 3C). Next, we used specific chemical inhibitors to identify the downstream pathway by which TLR-4 induces HTRA-1 expression. Inhibition of ERK, JNK, or p38 MAPK activity did not affect LPS-induced HTRA-1 mRNA expression (Figure 3D) or HTRA-1 production in the medium (Figure 3E), while inhibition of the PI3K pathway by LY294002 partially but significantly inhibited LPS-induced HTRA-1 synthesis ($P < 0.001$) (Figures 3D and E).

Inhibition of NF-κB significantly decreased LPS-induced HTRA-1 mRNA and protein expression (Figure 4A). Celastrol, a nonspecific NF-κB inhibitor that has been used as a treatment for RA in traditional Chinese medicine (35), efficiently inhibited LPS-induced HTRA-1 expression in a dose-dependent manner ($P < 0.001$) (Figure 4B). Knockdown of p65 using p65 short hairpin RNA markedly blocked HTRA-1 expression in RAW 264.7 cells after stimulation with LPS ($P < 0.01$) (Figure 4C). These data indicate that the classical NF-κB pathway regulates HTRA-1 expression in mouse macrophages.

Direct promotion of HTRA-1 gene expression in mouse macrophages by classical NF-κB. In order to determine if the classical NF-κB pathway directly regulates HTRA-1 gene transcription, we looked for potential transcription factor binding sites located within 2 kb upstream of the mouse HTRA-1 gene start site using Genomatix software suite version 2.4 (http://www.genomatix.de). In this region, there are 2 potential NF-κB binding sites: amino acid (aa) 347 (NF-κB binding site 1) and aa 1070 (NF-κB binding site 2) (Figure 4D). Using dual-luciferase reporter gene assays, we observed that HTRA-1 expression could be regulated at NF-κB binding site 1 (aa 347), but not at NF-κB binding site 2 (aa 1070) (Figure 4E), since HTRA-1 promoter fragment 1 (1–1515, which includes 2 NF-κB binding sites) and fragment 2 (1–698, which includes 1 NF-κB binding site [aa 347]) showed identical efficiency for HTRA-1 expression, but fragment 3 (1–292, which has no NF-κB binding site) did not. To further determine whether NF-κB acts directly on the HTRA-1 gene locus,

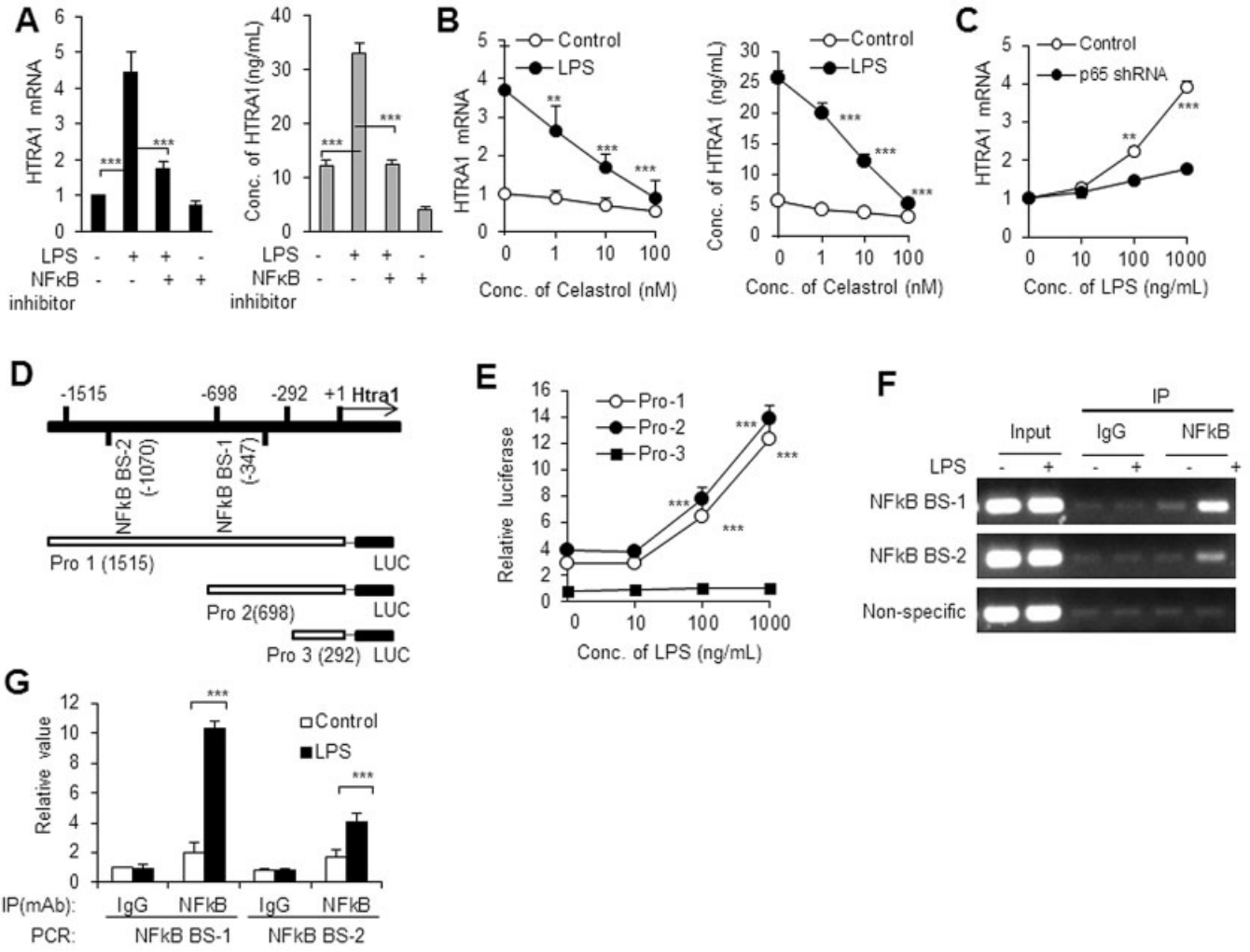

Figure 4. Induction of HTRA-1 expression by LPS is directly mediated by the classical NF-κB pathway in mouse macrophages. **A**, HTRA-1 mRNA and protein expression in RAW 264.7 cells pretreated with NF-κB inhibitor for 30 minutes and then cultured with LPS for an additional 24 hours. HTRA-1 mRNA expression was determined by real-time PCR, and HTRA-1 levels in culture medium were detected by ELISA. **B**, HTRA-1 mRNA and protein expression in RAW 264.7 cells pretreated with celastrol for 30 minutes and then cultured with LPS for an additional 24 hours. **C**, HTRA-1 mRNA expression in RAW 264.7 cells with ectopic overexpression of short hairpin RNA (shRNA) targeting p65. Cells were cultured with LPS for 24 hours. **D**, Schematic diagram of potential NF-κB binding sites (BS) in the HTRA-1 promoter (Pro) range and mouse HTRA-1 promoter constructs for the reporter gene and chromatin immunoprecipitation (ChIP) assays. **E**, Luciferase activity in RAW 264.7 cells cotransfected with a Fluc reporter plasmid containing different HTRA-1 promoter fragments and the internal control vector pRL-TK. Twenty-four hours after transfection, cells were stimulated with LPS for another 24 hours and luciferase activity was then determined. **F** and **G**, Binding to NF-κB binding sites, determined by PCR (**F**) and real-time PCR (**G**). After RAW 264.7 cells were treated with LPS for 6 hours, ChIP assays were performed and ChIP DNA was analyzed. Input DNA was used as an internal control, and data are shown as the relative fold increase over IgG control samples. Values in **A**, **B**, **C**, **E**, and **G** are the mean ± SD (n = 3 samples per group) and are representative of more than 2 independent experiments with similar results. ** = $P < 0.01$; *** = $P < 0.001$, versus control in **B** and **C**, versus promoter 3 in **E**, and versus the indicated groups in **A** and **G**. mAb = monoclonal antibody (see Figure 1 for other definitions).

we performed ChIP assays with anti–NF-κB mAb after cells were left unstimulated or stimulated with LPS. Although binding to both promoter sites increased, NF-κB predominantly bound to NF-κB binding site 1 (aa 347) when cells were stimulated with LPS, as determined by PCR (Figure 4F) and real-time PCR ($P < 0.001$) (Figure 4G). Taken together, these data indicate that LPS can promote HTRA-1 expression in mouse macrophages directly via the classical pathway of NF-κB activation. Furthermore, the NF-κB binding site aa 347

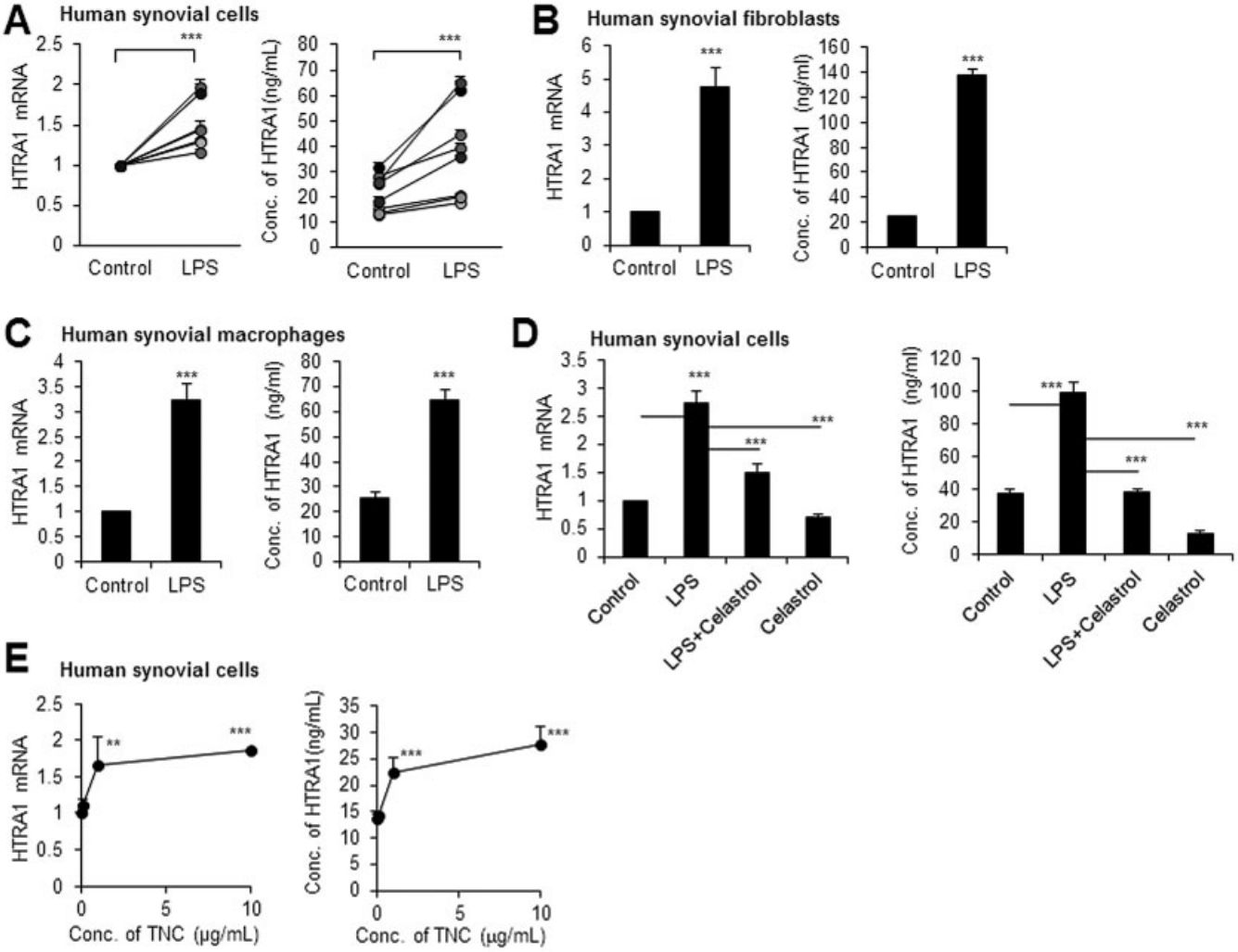

Figure 5. LPS promotes HTRA-1 gene expression in human cells via NF-κB. **A**, HTRA-1 mRNA levels and HTRA-1 protein concentrations in the culture media of freshly isolated human synovial cells obtained from 8 patients with rheumatoid arthritis (RA) and cultured with LPS for 24 hours. HTRA-1 mRNA levels were determined by real-time PCR, and HTRA-1 protein concentrations were measured by ELISA. **B** and **C**, HTRA-1 mRNA levels and HTRA1 protein concentrations in the culture media of freshly isolated human RA synovial fibroblasts (**B**) and human RA synovial macrophages (**C**) cultured with LPS for 24 hours. HTRA-1 mRNA levels were determined by real-time PCR, and HTRA-1 protein concentrations were measured by ELISA. **D**, HTRA-1 mRNA and protein levels in isolated human RA synovial cells precultured with NF-κB inhibitor (celastrol) for 30 minutes and then further cultured with LPS for 24 hours. HTRA-1 mRNA levels were determined by real-time PCR, and HTRA-1 protein concentrations in the culture media were measured by ELISA. Data in **B–D** are the mean ± SD (n = 3) and are representative of more than 2 independent experiments with similar results. **E**, HTRA-1 mRNA and protein levels in freshly isolated human synovial cells cultured with different concentrations of the Toll-like receptor 4 ligand tenascin-C (TN-C) for 24 hours. Values are the mean ± SD (n = 3 samples per group). ** = $P < 0.01$; *** = $P < 0.001$, versus control in **B**, **C**, and **E** and versus the indicated groups in **A** and **D**. See Figure 1 for other definitions.

in the HTRA-1 promoter range is critical for LPS regulation of HTRA-1 expression.

Regulation of HTRA-1 expression in human synovial cells by TLR-4 ligands. To assess whether the findings in mouse cells were reproducible in humans, we used freshly isolated total human RA synovial cells to determine the role of TLR ligands in HTRA-1 expression. HTRA-1 mRNA expression and protein production were significantly higher in LPS-treated cells than in controls (Figure 5A), as determined by real-time PCR and ELISA, respectively. Moreover, LPS significantly induced HTRA-1 mRNA and protein expression in human synovial fibroblasts ($P < 0.01$) (Figure 5B) and synovial monocyte/macrophages ($P < 0.01$) (Figure 5C)

isolated from RA patients. Celastrol efficiently inhibited LPS-induced HTRA-1 expression in human synovial cells ($P < 0.001$) (Figure 5D). TN-C, an endogenous TLR-4 activator that mediates persistent synovial inflammation and tissue destruction in RA (10), induced HTRA-1 mRNA expression as well as HTRA-1 production in human synovial cells in a dose-dependent manner (Figure 5E). These data indicate that TLR-4 ligands, including LPS and TN-C, have the ability to induce HTRA-1 expression in human synovial fibroblasts and monocyte/macrophages via the classical NF-κB pathway.

DISCUSSION

The findings of the present study show that TLR-4 ligands significantly exacerbate arthritis and induce high levels of HTRA-1 expression in vivo and in vitro by activating the classical NF-κB pathway. These results indicate that TLR-4 activation caused by infections or enhanced endogenous ligands like TN-C may have a significant impact on the disease process through HTRA-1 expression in addition to the previously recognized inflammation pathways. Blocking HTRA-1 activity significantly reversed LPS-promoted incidence and severity of arthritis in the mouse model of CIA. Taken together, these findings reveal new molecular mechanisms in the pathogenesis of arthritis and emphasize the importance of infections and endogenous TLR-4 ligands in the pathogenesis of arthritis through protease pathways.

TLR ligands such as LPS and TN-C, as well as other infectious agents, have been shown to play a role in the pathogenesis of RA (4,6,7,9,10). TN-C, which is specifically expressed in areas of inflammation and tissue damage, mediates persistent synovial inflammation and tissue destruction in arthritic joint disease (10). Our data indicate that LPS and TN-C induce the expression of the tissue-destructive protease HTRA-1 in fibroblasts and macrophages, two major HTRA-1–producing cells in RA (20). Importantly, LPS induced significantly higher HTRA-1 expression in the joints and greatly increased the incidence and severity of arthritis in the mouse model of CIA. The LPS-induced HTRA-1 expression was supported by decreased TSC-2 expression, which was directly regulated by HTRA-1 (33). Consistent with the observations in mouse cells and the mouse model, stimulation with LPS or TN-C induced significantly higher HTRA-1 mRNA and protein expression in freshly isolated synovial fibroblasts and monocyte/macrophages from RA patients compared to unstimulated cells. Importantly, blocking HTRA-1 using antibody partially but significantly reversed the pathogenesis of arthritis in LPS-treated mice with CIA. Thus, the regulation of HTRA-1 expression by LPS is of clinical relevance. Together with the previous findings that LPS also significantly induces other matrix-degrading enzymes such as MMPs, the involvement of LPS-induced degrading enzymes in RA pathogenesis should be recognized in addition to its strong inflammatory effects.

With molecular and biochemical assays, we demonstrated that the classical NF-κB pathway directly mediates LPS-induced HTRA-1 expression. In this pathway, TLR-4 activation results in preferential binding of p65 to aa 347 in the HTRA-1 promoter, which subsequently induces HTRA-1 transcription, as supported by the results of dual-luciferase reporter assays and ChIP assays. Taken together, these data showed that the classical NF-κB pathway participates in regulating TLR-mediated HTRA-1 expression in macrophages.

Furthermore, our findings may be of significance in the understanding and treatment of other HTRA-1–related processes, such as AMD, cancer, and aging. One study showed that loss of HTRA-1 in ovarian and gastric cancers contributes to chemoresistance (27). Jones et al demonstrated that increased HTRA-1 alone is sufficient to cause polypoidal choroidal vasculopathy and is a risk factor for choroidal neovascularization (24). Therefore, we speculate that regulation of HTRA-1 expression by TLR-4 ligands via the classical NF-κB pathway may also be important in other HTRA-1–related pathologic processes and may have a broad range of therapeutic applications.

It is worth noting that TNFα and IL-1β, which are important pathogenic factors in RA (36,37), failed to induce HTRA-1 expression in MEFs and even slightly inhibited HTRA-1 expression in macrophages. In addition, anti-TNFα mAb failed to block the inducing effect of LPS on HTRA-1 expression in vitro (data not shown). Taken together, these data indicate the unique and direct role of LPS in HTRA-1 induction in macrophages and fibroblasts. It has been reported that TNFα, IL-1β, and LPS share some common signal pathways, including NF-κB and others; however, the efficiency of induction may be different (38,39). The differential effects of these two cytokines and LPS suggest that TNFα and IL-1β may even activate additional signal transduction pathways that inhibit HTRA-1 expression. Which pathways are involved in the slightly reduced HTRA-1 expression in TNFα-treated macrophages requires further research.

In summary, LPS significantly increases HTRA-1 expression in fibroblasts and monocyte/macrophages

directly via the classical NF-κB pathway. This study offers new insights into the regulation of HTRA-1 expression via LPS/TLR-4 and the role of LPS/TLR-4–induced HTRA-1 in the pathogenesis of RA.

ACKNOWLEDGMENTS

The authors wish to thank Drs. Nickolas Nahm and Hanhan Li for their kind review of the manuscript, Mrs. Jing Wang, Mr. Yabing Liu, and Dr. Xiaoqiu Liu for expert technical assistance, Mrs. Qinghuan Li and Mrs. Jianxia Peng for excellent laboratory management, and Mr. Hongfei Wu for outstanding animal husbandry.

AUTHOR CONTRIBUTIONS

All authors were involved in drafting the article or revising it critically for important intellectual content, and all authors approved the final version to be published. Drs. Hou and Zhao had full access to all of the data in the study and take responsibility for the integrity of the data and the accuracy of the data analysis.

Study conception and design. Hou, Lin, L. Zhu, Liu, Hu, J. Shi, Yang, X. Shi, M. Zhu, Godley, Wang, Li, Zhao.

Acquisition of data. Hou, Lin, L. Zhu, Liu, Hu, J. Shi, Yang, X. Shi, M. Zhu, Godley, Wang, Li, Zhao.

Analysis and interpretation of data. Hou, Lin, L. Zhu, Liu, Hu, J. Shi, Yang, X. Shi, M. Zhu, Godley, Wang, Li, Zhao.

REFERENCES

1. Brennan FM, McInnes IB. Evidence that cytokines play a role in rheumatoid arthritis. J Clin Invest 2008;118:3537–45.
2. Al-Katma MK, Bissada NF, Bordeaux JM, Sue J, Askari AD. Control of periodontal infection reduces the severity of active rheumatoid arthritis. J Clin Rheumatol 2007;13:134–7.
3. Ebringer A, Rashid T. Rheumatoid arthritis is an autoimmune disease triggered by Proteus urinary tract infection. Clin Dev Immunol 2006;13:41–8.
4. Abdollahi-Roodsaz S, Joosten LA, Helsen MM, Walgreen B, van Lent PL, van den Bersselaar LA, et al. Shift from Toll-like receptor 2 (TLR-2) toward TLR-4 dependency in the erosive stage of chronic streptococcal cell wall arthritis coincident with TLR-4–mediated interleukin-17 production. Arthritis Rheum 2008;58: 3753–64.
5. Abdollahi-Roodsaz S, Joosten LA, Koenders MI, Devesa I, Roelofs MF, Radstake TR, et al. Stimulation of TLR2 and TLR4 differentially skews the balance of T cells in a mouse model of arthritis. J Clin Invest 2008;118:205–16.
6. Roelofs MF, Boelens WC, Joosten LA, Abdollahi-Roodsaz S, Geurts J, Wunderink LU, et al. Identification of small heat shock protein B8 (HSP22) as a novel TLR4 ligand and potential involvement in the pathogenesis of rheumatoid arthritis. J Immunol 2006;176:7021–7.
7. Sacre SM, Andreakos E, Kiriakidis S, Amjadi P, Lundberg A, Giddins G, et al. The Toll-like receptor adaptor proteins MyD88 and Mal/TIRAP contribute to the inflammatory and destructive processes in a human model of rheumatoid arthritis. Am J Pathol 2007;170:518–25.
8. Huang QQ, Pope RM. The role of Toll-like receptors in rheumatoid arthritis. Curr Rheumatol Rep 2009;11:357–64.
9. Cutolo M, Picasso M, Ponassi M, Sun MZ, Balza E. Tenascin and fibronectin distribution in human normal and pathological synovium. J Rheumatol 1992;19:1439–47.
10. Midwood K, Sacre S, Piccinini AM, Inglis J, Trebaul A, Chan E, et al. Tenascin-C is an endogenous activator of Toll-like receptor 4 that is essential for maintaining inflammation in arthritic joint disease. Nat Med 2009;15:774–80.
11. Clausen T, Southan C, Ehrmann M. The HtrA family of proteases: implications for protein composition and cell fate. Mol Cell 2002;10:443–55.
12. Tsuchiya A, Yano M, Tocharus J, Kojima H, Fukumoto M, Kawaichi M, et al. Expression of mouse HtrA1 serine protease in normal bone and cartilage and its upregulation in joint cartilage damaged by experimental arthritis. Bone 2005;37:323–36.
13. Polur I, Lee PL, Servais JM, Xu L, Li Y. Role of HTRA1, a serine protease, in the progression of articular cartilage degeneration. Histol Histopathol 2010;25:599–608.
14. Hoy B, Lower M, Weydig C, Carra G, Tegtmeyer N, Geppert T, et al. Helicobacter pylori HtrA is a new secreted virulence factor that cleaves E-cadherin to disrupt intercellular adhesion. EMBO Rep 2010;11:798–804.
15. Vierkotten S, Muether PS, Fauser S. Overexpression of HTRA1 leads to ultrastructural changes in the elastic layer of Bruch's membrane via cleavage of extracellular matrix components. PLoS One 2011;6:e22959.
16. An E, Sen S, Park SK, Gordish-Dressman H, Hathout Y. Identification of novel substrates for the serine protease HTRA1 in the human RPE secretome. Invest Ophthalmol Vis Sci 2010;51: 3379–86.
17. Zumbrunn J, Trueb B. Primary structure of a putative serine protease specific for IGF-binding proteins. FEBS Lett 1996;398: 187–92.
18. Zhang L, Lim SL, Du H, Zhang M, Kozak I, Hannum G, et al. High temperature requirement factor A1 (HTRA1) gene regulates angiogenesis through transforming growth factor-β family member growth differentiation factor 6. J Biol Chem 2012;287:1520–6.
19. Hu SI, Carozza M, Klein M, Nantermet P, Luk D, Crowl RM. Human HtrA, an evolutionarily conserved serine protease identified as a differentially expressed gene product in osteoarthritic cartilage. J Biol Chem 1998;273:34406–12.
20. Grau S, Richards PJ, Kerr B, Hughes C, Caterson B, Williams AS, et al. The role of human HtrA1 in arthritic disease. J Biol Chem 2006;281:6124–9.
21. Wu J, Liu W, Bemis A, Wang E, Qiu Y, Morris EA, et al. Comparative proteomic characterization of articular cartilage tissue from normal donors and patients with osteoarthritis. Arthritis Rheum 2007;56:3675–84.
22. Weger M, Renner W, Steinbrugger I, Kofer K, Wedrich A, Groselj-Strele A, et al. Association of the HTRA1 -625G>A promoter gene polymorphism with exudative age-related macular degeneration in a Central European population. Mol Vis 2007;13: 1274–9.
23. Mullany SA, Moslemi-Kebria M, Rattan R, Khurana A, Clayton A, Ota T, et al. Expression and functional significance of HtrA1 loss in endometrial cancer. Clin Cancer Res 2011;17:427–36.
24. Jones A, Kumar S, Zhang N, Tong Z, Yang JH, Watt C, et al. Increased expression of multifunctional serine protease, HTRA1, in retinal pigment epithelium induces polypoidal choroidal vasculopathy in mice. Proc Natl Acad Sci U S A 2011;108:14578–83.
25. Bakay M, Zhao P, Chen J, Hoffman EP. A web-accessible complete transcriptome of normal human and DMD muscle. Neuromuscul Disord 2002;12 Suppl 1:S125–41.
26. Murwantoko, Yano M, Ueta Y, Murasaki A, Kanda H, Oka C, et al. Binding of proteins to the PDZ domain regulates proteolytic activity of HtrA1 serine protease. Biochem J 2004;381(Pt 3): 895–904.
27. Chien J, Aletti G, Baldi A, Catalano V, Muretto P, Keeney GL, et al. Serine protease HtrA1 modulates chemotherapy-induced cytotoxicity. J Clin Invest 2006;116:1994–2004.
28. Ma H, Liu G, Ding W, Wu Y, Cai L, Zhao Y. Diabetes-induced

alteration of F4/80+ macrophages: a study in mice with streptozotocin-induced diabetes for a long term. J Mol Med (Berl) 2008;86:391–400.
29. Sun C, Sun L, Ma H, Peng J, Zhen Y, Duan K, et al. The phenotype and functional alterations of macrophages in mice with hyperglycemia for long term. J Cell Physiol 2012;227:1670–9.
30. Inglis JJ, Notley CA, Essex D, Wilson AW, Feldmann M, Anand P, et al. Collagen-induced arthritis as a model of hyperalgesia: functional and cellular analysis of the analgesic actions of tumor necrosis factor blockade. Arthritis Rheum 2007;56:4015–23.
31. Williams RO. Collagen-induced arthritis as a model for rheumatoid arthritis. Methods Mol Med 2004;98:207–16.
32. Jia Y, Takimoto K. GATA and FOG2 transcription factors differentially regulate the promoter for Kv4.2 K^+ channel gene in cardiac myocytes and PC12 cells. Cardiovasc Res 2003;60:278–87.
33. Campioni M, Severino A, Manente L, Tuduce IL, Toldo S, Caraglia M, et al. The serine protease HtrA1 specifically interacts and degrades the tuberous sclerosis complex 2 protein. Mol Cancer Res 2010;8:1248–60.
34. Mendes Sdos S, Candi A, Vansteenbrugge M, Pignon MR, Bult H, Boudjeltia KZ, et al. Microarray analyses of the effects of NF-κB or PI3K pathway inhibitors on the LPS-induced gene expression profile in RAW264.7 cells: synergistic effects of rapamycin on LPS-induced MMP9-overexpression. Cell Signal 2009;21:1109–22.
35. Lee JH, Koo TH, Yoon H, Jung HS, Jin HZ, Lee K, et al. Inhibition of NF-κB activation through targeting IκB kinase by celastrol, a quinone methide triterpenoid. Biochem Pharmacol 2006;72:1311–21.
36. Gonzalez-Gay MA, Gonzalez-Juanatey C. Rheumatoid arthritis: obesity impairs efficacy of anti-TNF therapy in patients with RA. Nat Rev Rheumatol 2012;8:641–2.
37. Lampa J, Westman M, Kadetoff D, Agreus AN, Le Maitre E, Gillis-Haegerstrand C, et al. Peripheral inflammatory disease associated with centrally activated IL-1 system in humans and mice. Proc Natl Acad Sci U S A 2012;109:12728–33.
38. Kant S, Swat W, Zhang S, Zhang ZY, Neel BG, Flavell RA, et al. TNF-stimulated MAP kinase activation mediated by a Rho family GTPase signaling pathway. Genes Dev 2011;25:2069–78.
39. Weber A, Wasiliew P, Kracht M. Interleukin-1 (IL-1) pathway. Sci Signal 2010;3:cm1.